Archives of Computational Methods in Engineering (2021) 28:1–13
https://doi.org/10.1007/s11831-019-09366-4

ORIGINAL PAPER

Computational Nuclei Segmentation Methods in Digital Pathology: A Survey

Tomohiro Hayakawa[1] · V. B. Surya Prasath[2,3,4,5] · Hiroharu Kawanaka[1] · Bruce J. Aronow[2,3,4] · Shinji Tsuruoka[1]

Received: 14 March 2019 / Accepted: 30 September 2019 / Published online: 8 October 2019

Abstract
Pathology is an important field in modern medicine. In particular, the step of nuclei segmentation is an important step in cancer analysis, diagnosis, and grading because cancer analysis, diagnosis, classification, and grading are highly dependent on the quality (accuracy) of nuclei segmentation. In the conventional cancer diagnosis, pathologists analyze biopsies to make diagnostic and prognostic assessments, mainly based on the cell morphology and architecture distribution. In recent years, computerized approaches are rapidly developing in the field of digital pathology, and applications related to nuclei detection, segmentation and classification are increasing. These approaches will play an important role of minimizing human intervention, integrating relevant second opinions, and providing traceable clinical information. In the past, much effort has been devoted to automation of nuclei segmentation and methods to deal with nuclei complex structure. This review provides the summary of the techniques and experimental materials used for nuclei segmentation.

1 Introduction

Cancer is one of the leading causes of mortality worldwide. In these years, the number of deaths due to cancer continues to increase, and in 2016 it became approximately 30% of the cause of death in Japan. In the field of histopathology, the evaluation of the disease status is based on cell nuclei information of the tissue images, and appropriate treatments are required for each cancer and grade. Therefore, it is necessary to extract the region of cell nuclei accurately. However, cells have complex structures (see Fig. 1), and they come from various situations [1]. For that reason, manual analysis is difficult for pathologists. Digital pathology and microscopy images play a significant role in decision making for disease diagnosis, since they can provide extensive information for Computer-Aided Diagnosis (CAD). It realizes a quantitative analysis of digital images with a high throughput processing rate.

Currently, there are several review papers on automated pathological image analysis. The review paper published by Gurcan et al. [2] summarized the CAD system technologies for image analysis, which covers preprocessing, nuclei segmentation and gland segmentation, feature extraction, and classification. Irshad et al. [1] provided a survey on the methods for nuclei detection, segmentation and classification in hematoxylin and eosin (H&E) and immunohistochemistry (IHC) stained histopathology images. Xing et al. have proposed the review on robust nuclei/cells detection and segmentation in digital pathology and microscopy images [3]. According to [2], despite a lot of automated methods for nuclei segmentation have been proposed, it is difficult for pathologists to find a good one to use since there are plenty of competing segmentation methods with different capbilities.

In this survey, we focus on automatic computational methods for nuclei/cells segmentation and review some of the important techniques published in the past years. Also, we also surveyed commonly used modality for staining, preprocessing and some basic methods. The organization of this paper is as follows. Section 2 introduces the imaging modalities in histopathology and emphasizes the challenges

✉ V. B. Surya Prasath
surya.prasath@cchmc.org; prasatsa@uc.edu

[1] Department of Electrical and Electronic Engineering, Mie University, Tsu, Mie, Japan

[2] Division of Biomedical Informatics, Cincinnati Children's Hospital Medical Center, Cincinnati, OH 45229, USA

[3] Department of Pediatrics, University of Cincinnati, Cincinnati, OH 45267, USA

[4] Department of Biomedical Informatics, College of Medicine, University of Cincinnati, Cincinnati, OH 45267, USA

[5] Department of Electrical Engineering and Computer Science, University of Cincinnati, Cincinnati, OH 45221, USA

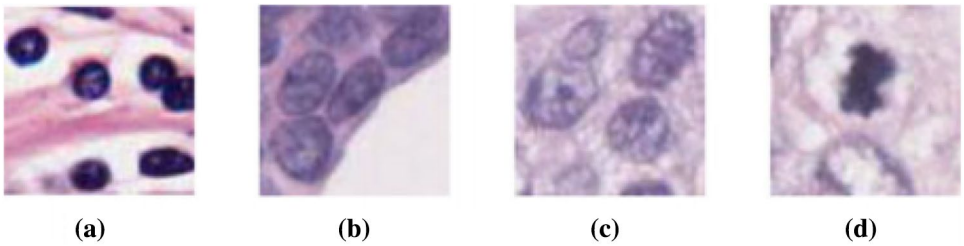

Fig. 1 Different types of nuclei. **a** LN, **b** EN, **c** EN (cancer), **d** EN (mitosis)

Table 1 Abbreviations used in the survey

Symbol	Description	Symbol	Description	Symbol	Description
Acc	Accuracy	ACMs	Active contour models	ALL	Acute lymphoblastic leukemia
CAD	Computer-aided diagnosis	CNN	Convolutional neural network	CS	Correctly segmentation
DC	Dice coefficient	DP	Dynamic programming	EM	Expectation maximization
FCM	Fuzzy C-means	FN	False negative	FPR	False positive rate
GBM	Glioblastoma	GC	Graph cut	GMM	Gaussian mixture models
H&E	Hematoxylin and eosin	IHC	Immunohistochemistry	LoG	Laplacian of Gaussian
MO	Morphological operation	Ncut	Normalized cut	OR	Overall accuracy rate
OS	Over segmentation	PPV	Positive predictive value	RBC	Red blood cells
ROI	Region of interest	RI	Rand index	Sen	Sensitivity
TMA	Tissue microscopy array	TNR	True negative rate	TPR	True positive rate
US	Under segmentation	WBC	White blood cells	WSI	Whole-slide imaging

in computational nuclei segmentation. Section 3 provides the methods of preprocessing and segmentation in histopathology. Section 4 addresses the challenges and clarifies the gap in nuclei segmentation. We show future directions and problems in nuclei segmentation and conclude with a discussion. A list of symbols and notation commonly used in this survey paper is shown in Table 1.

2 Basics of Digital Pathology and Challenges

2.1 Staining and Image Modality in Digital Pathology

In digital pathology, the microscopic examination of surgical specimen or biopsy is conducted onto glass slides to study cancer expression, genetic progression, and cellular morphology for cancer diagnosis and prognosis. For tissue constituents visualization under a microscope, tissue images are dyed with one or more stains.

H&E staining is one of the staining methods used worldwide in the field of pathology. H&E staining has been used by pathologists for a long time and is still widely used for visualization of tissue features under a microscope. Hematoxylin stains nuclei in dark blue color, and eosin stains other structures (cytoplasm, stroma, etc.) with a pink color

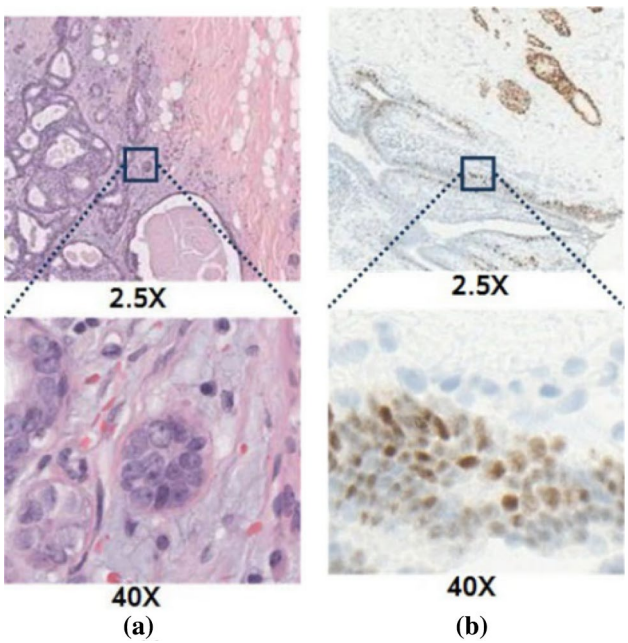

Fig. 2 Examples of hematoxylin and eosin and IHC staining images. **a** H&E. **b** IHC

(Fig. 2a), [1]. Nuclei are diagnostically meaningful to indicate benign or malignant cancer.

Immunohistochemical (IHC) is a type of the staining methods, which is usually used as a cancer diagnosis to

determine whether the obtained tissue is benign or malignant. Figure 2b shows an example of IHC staining images. IHC can help to determine the region of a tumor and we can select an appropriate treatment by investigating the appearance of specific proteins.

Papanicolaou staining is a typical staining method for morphological observation. This method is also an important method like H&E staining. Papanicolaou staining method is almost the same as H&E staining for the cell nuclei, but the cytoplasm can be represented by three kinds of colors. However, this method requires many steps to acquire results. It means that the accuracy of the obtained result may or may not depend on facilities. The normalization of staining is required in the method. They are basic staining methods to study for cancer diagnosis and prognosis under a microscope.

2.2 Challenges in Nuclei Segmentation

There are various types of nuclei, and it depends on several factors such as nuclide, malignant tumor, their life cycles, etc. In the case of white blood cells, there are several classes, e.g., Neutrophils, Eosinophils, Lymphocytes. For instance, lymphocytes are essential for immune cells that occupy most of the white blood cells. The variety of blood cells makes nuclei segmentation very difficult.

Automated nuclei segmentation is one of the well-studied topics in the field of digital pathology, and many methods have already been proposed. However, these proposed methods are not perfect and cannot be applied to all types of histopathology images due to variability caused by factors in slide preparation (dyes concentration, damages of the given tissue sample, etc.) and image acquisition (presence of digital noise, specific features of the slide scanner, etc.). Furthermore, nuclei in the given image are sometimes overlapped each other and distributed non-uniformity. All of them affect not only nuclei segmentation but also prognostic prediction and diagnosis. All image processing approaches have to overcome these issues, and also should be robust methods to keep accuracy high in any situation.

3 Methods for Nuclei Segmentation

Nuclei segmentation is an important step in cancer diagnosis and grading, prognostic prediction. Since tissue properties are different in each disease stage, the information of nuclei is critical for evaluating disease progress and its severity. Therefore, various approaches are required at each step in the processing. Nuclei segmentation mainly consists of two important steps, preprocessing and segmentation. We next introduce the standard preprocessing methods that are used in nuclei segmentation methods for histopathology images. We further review salient nuclei segmentation methods that were published in the recent years.

3.1 Preprocessing

To extract expected information from given images, preprocessing is necessary and usually performed. In the histopathological image processing, the structure and status of cells differ depending on each disease. There are many types of preprocessing methods, and some of them consist of the combination of basic techniques.

3.1.1 Denoising

In this process, filter techniques are often used to remove the noise in the images. Depending on the purpose, it is possible to obtain the appropriate results by emphasizing the feature (expansion/contraction, etc.) and blurring to reduce the noise component (averaging/median, etc.). For instance, a median filter was used in [4, 5]. A median filter can remove noise without blurring contours of desired objects. Understanding feature(s) of each filtering technique is essential in preprocessing.

3.1.2 Color Processing

In image processing, color plays an important role. The outline of what is drawn in the image can be recognized by color. Images give different impressions only by changing the color space. The color information serves as an index for dividing an area and is a useful feature for distinguishing objects in the image. By converting the color system of the given image, it is possible to make it easy to obtain the intended information. It is also possible to extract the area for analysis and diagnosis from the brightness gradient by extracting pixel values. Generally, RGB color space can be converted into several color space.

CIE L*a*b* color system is designed to approximate human vision. In general, the human sense tends to be proportional to the logarithm of the stimulus value, not proportional to the stimulus value itself. The sense of brightness is no exception. In [6], they transform the histopathology images from the RGB to the CIELAB color space, which is based on human eye perception, to exploit this property. In the three L*a*b*, defined by CIE, the a* component, which divides the color axis between magenta and green, was used for discrimination. A double-threshold was used on the a* channel to discriminate between connective tissue, background and myocytes [6].

Conversion of a color image is quite a common way in digital image processing. HSV (Hue, Saturation, Value) transform is widely used in image analysis methods for segmentation [7]. HSV color system is more suitable to convey

color information compared to RGB color model, and not vulnerable to illumination. Hue information in the HSV model is a significant feature for cell segmentation because cell nuclei and cytoplasm will absorb different coloring agents, [4]. There are some studies using not only one of the HSV color factors [7, 8] but also all factors. There is also HSI color space, which is similar to HSV color space [9].

3.1.3 Seeds Detection

In segmentation, detection, and classification of cells and nuclei, they are not necessarily independent. Therefore, it is difficult to directly segment cells from microscopic images when they are in contact with each other. In carrying out various treatments, separating contacting cells are required. This process needs the identification of seed points where there is one marker per cell. For instance,

Al-Kofahi et al. identified the seed point of cells with the multiscale Laplacian of Gaussian (LoG) filter [10]. LoG filter [11] consists of Gaussian and Laplacian filters. After smoothing the image with the Gaussian filter(s) to reduce noise, the boundary is extracted with Laplacian filter. Since Laplacian filter acts as a quadratic differential operation(s), noise is easily emphasized, but it is reduced by smoothing the image beforehand with Gaussian filters.

Parvin et al. [12] detected cell seed points by a method using repetitive voting technique. Xin Qi et al. [13] mentioned the views on the problems of these methods and proposed a new method based on parallel seed detection and repulsive level sets.

3.1.4 Color Normalization

Image processing specialists often compare some digital images that were captured under different light condition. In such cases, it is required to convert the mean and standard variation of the image brightness value. Such techniques are usually called color normalization, and many color normalization techniques have been proposed. For instance, histograms or quantile normalization are used for color normalization. In the case of color image, distributions of three color channels are often normalized separately. By adjusting the unevenness of brightness with these techniques, the performance of the subsequent processing can be improved. Most segmentation and detection methods use the RGB color system, but it is not a perceptual color model. For that reason, other color models such as HSV, CIE L*a*b*, and Luv are usually used.

3.1.5 Region of Interest (ROI) Detection

The region of Interest (ROI) means the area selected for filter or other operations. The ROI is defined and expressed by a binary mask. This is an image with the same size as the target image, The pixel values that correspond to ROI are set to 1, and other regions are set to 0. In some cases, the regions are defined based on the area that consists of polygons enclosed by consecutive pixels, or by intensity ranges.

In some frameworks, noise reduction and ROI detection are performed simultaneously. For example, the ROIs were selected by excluding regions with little content and noise at the preprocessing step [14]. For nuclei level feature computation, noise reduction is succeeded by ROI detection to determine the nuclei region [15].

Thresholding is common for ROI detection. Lee et al. [16] normalized the ROI corresponding to the nuclei region from the microscopic image before identifying it. After normalization, using the Otsu thresholding method [17], ROI was detected from the image by combining global thresholding and local thresholding.

3.2 Segmentation Methods

3.2.1 Thresholding

Thresholding is the easiest method for image segmentation. The basic idea of thresholding is to replace each pixel in the image with a white pixel if the pixel value exceeds a certain threshold and replace it with a black pixel if not. There are roughly two methods for determining the threshold T to be used. The first method is a global threshold, and the other is a local threshold approach. A global threshold value can be determined by using computational methods like the Otsu method. A histogram of the entire image is obtained, and then a threshold value is determined for the whole image from the result of the histogram. In the local (adaptive) threshold approach, the average of pixel values and the standard deviation around the target pixel to be binarized, and the threshold value is determined considering them. After this, the given image is converted into a binary image, and we can extract desired objects easily from the obtained binary image.

Thresholding approach works well and is the most efficiently conducted in HSV color space. There are variety of variants on nuclei segmentation using thresholding [8, 18–24, 26–33].

For instance, Lu et al. introduced the segmentation method by using the local (adaptive) thresholding in cutaneous images [18]. Gadgil et al. used the same approach as the preprocessing for the nuclei segmentation [20]. Thus, thresholding is very important as not only merely segmentation but also preprocessing for applicative segmentation. Table 2 provides the comparison of different thresholding methods for nuclei segmentation methods along with the

Table 2 Summary of thresholding based nuclei segmentation methods for histopathological images

Refs.	Dataset	Preprocessing and segmentation	Segmentation results
[8]	70 blood smear images	Otsu thresholding, HSV transform	–
[18]	30 H&E cutaneous images	Local region adaptive threshold selection module	SEN: 88.11%, PPV: 80.02%
[19]	3D confocal images	Hough transform, median filter, adaptive thresholding	–
[20]	Rat kidney images	Adaptive thresholding, shape-fitting	–
[21]	FISH breast images	Adaptive gamma correction with weighting distribution (AGCWD) Otsu thresholding	–
[22]	25 Pap pleural fluid images	Medial filter, Otsu thresholding, MO	SEN: 94%
[23]	60 WBCs images	Otsu thresholding, marker controlled watershed, MO	Acc: 90.2% (normal), 82.4% (leukemia)
[24]	39 H&E cervical images	Adaptive thresholding, ellipse fitting, Adaptive Nucleus Shape Modeling (ANSM)	–
[25]	ISBI-2014: 945 synthetic and 16 Pap smear slide images ISBI-2015: 17 real extended depth of field images	Adaptive thresholding, local thresholding	ISBI-14: DC: 89.7 $\pm$ 7.5, FN: 13.7 $\pm$ 1.94%, TP: 88.2 $\pm$ 9.7%, FP: 0.2 $\pm$ 0.3%, ISBI-15: DC: 87.9 $\pm$ 8.7%, FN: 43.4 $\pm$ 16.8%, TP: 87.7 $\pm$ 12.3%, FN: 0.1 $\pm$ 0.1%
[26]	150 H&E GBM images	Thresholding, smoothing	–
[27]	88 Wright's staining blood smear images	Otsu thresholding, mathematical morphing	Neutrophil: 55%, Basophil: 60%, Eosinophil: 87.5%, Lymphocyte: 100%, Monocyte: 90%
[28]	150 Type P63 non-counter stained ovarian images	Thresholding, watershed	–
[29]	365 blood images (dataset1), 242 blood images (dataset2)	Discrete wavelet transform, Poisson distribution, morphological filtering	Similarity measures: 85.1% (dataset1), Similarity measures: 83.5% (dataset2)
[30]	Phase contrast images	H-maxima transform, marker controlled watershed, Otsu thresholding, MO	Precision: 93.8%, recall: 92.2%
[31]	H&E stomach images	k-means clustering, thresholding	–
[32]	15 multi-layer cervical cell volumes	Thresholding, EM algorithm, GMM	DC: 86.1, FN object: 35.2%, TP pixels: 87.4%, FP pixels: 0.1%
[33]	2078 glioma nuclei images	Optimal thresholding, level set, hierarchical mean shift	–

results obtained. We highlight the prominent preprocessing steps utilized as well.

3.2.2 Watershed

Watershed is one of the segmentation methods and used in many papers [23, 28, 30, 34–41]. As the first step of this approach, specific pixels called makers are determined, and then the markers are expanded gradually like flooding. In Watershed, the surrounding regions of makers are called catchment basin, and each pixel value is treated as a local topography. Catchment basins are separated topographically from adjacent catchment basins by maximum altitude lines called watershed lines. It allows classifying every point of a topographic surface as either belonging to the catchment basin associated with one of the local minimum or to the watershed line. Details about watershed approach can be found in [42]. The Watershed transformation is usually computerized on the gradient image instead of the intensity image.

Segmentation using the watershed transform works well if the position of the front object and the background can be identified or marked. A marker-controlled watershed is used in [34, 35]. This algorithm considers the input image as a topographic surface and simulates its flooding from specific seed points or markers. Table 3 provides the details of watershed based approaches. The highest accuracy was reported by Rajyalakshmi et al. [38], wherein a modified the marker-controlled watershed obtained the segmentation accuracy of 95.79 (normal), 95.56 (invasive) %.

3.2.3 Morphological Operations

Morphology is a set-theoretic approach that considers an image as the elements of a set and process images as geometrical shapes. This approach is defined by the operation(s) between the processing target images and the structuring

Table 3 Summary of watershed based nuclei segmentation methods for histopathological images

Refs.	Dataset	Preprocessing and segmentation	Segmentation results
[34]	39 H&E breast images	Marker controlled watershed	DC > 0.8
[35]	19 H&E breast images	Marker controlled watershed	Radial symmetry markers: 79.2%, regional minima markers: 79.6%
[36]	52 DAB colorectal TMA and WSI	Watershed	OR: 80.3%
[37]	Ki-67 breast images	Watershed	–
[38]	120 H&E breast images	Modified marker controlled watershed, MO, Otsu thresholding, Hough transform	Acc: 95.79% (normal), 95.56% (invasive)
[39]	H&E breast images	Marker controlled watershed	Precision: 92%, recall: 92%
[40]	Human breast TMA, MCF-10A, Mouse Embryos	Oriented watershed, DP	–
[41]	423 H&E lymphoma images	Watershed, hierarchical k-means clustering	–

elements. The two basic morphological operations are Erosion and Dilation. The effect of these operations is to shrink (enlarge) the boundaries of foreground pixels. Two other major operations in morphological approach are Opening and Closing. The opening operation is an erosion of an image followed by dilation, and it eliminates small objects and lines. Closing is a dilation of an image followed by erosion, and it fills small holes in the image. White and Black Top-Hat Transforms are two other operations derived from morphology. They allow extracting small elements and details from given images. The white top-hat transform is defined as the difference between the original image and the opening images. The Black Top-Hat Transform is defined as the difference between the original image and the closing images. There are methods that exploit morphological operations along with other other techniques such as thresholding [22, 43], level sets [7, 48], k-means clustering [44, 45], and PCA [45], Hough transform [47]. Table 4 provides an overview of these morphological techniques in nuclei segmentation. As can be seen, highest accuracy was obtained by a hybrid method that uses anisotropic diffusion filtering, and morphological toggle filter [46] on two different datasets.

3.2.4 Active Contour Models (ACMs) and Level Sets

Active contour models (ACMs) or deformable models and these are widely used in image segmentation [49–54]. In the approaches, a segmentation boundary is expressed as deformable splines, and an energy function, which is defined by gradient information, determines the shapes by seeking to minimize the energy function [62]. In case of nuclei segmentation, the contour points that yield the minimum energy level form the boundary of nuclei. The energy function is often defined to penalize discontinuity in the curve shape and gray-level discontinuity along the contour [63].

There is two main form of ACMs. An explicit parametric representation of the contour, which is called Snakes [64], is robust to image noise and boundary gaps as it constrains the extracted boundaries to be smooth. It is, however, difficult

Table 4 Summary of mathematical morphology filters based nuclei segmentation methods for histopathological images

Refs.	Dataset	Preprocessing and segmentation	Segmentation results
[7]	15 computational brain tumor cluster (CBTC) images	HSV transform, level set to V component, MO	–
[43]	24 H&E breast images	Adaptive thresholding, MO	–
[44]	20,148 Pap smear cell images	k-means clustering, MO, polar transform	–
[45]	132 H&E prostate TMA	k-means clustering, morphological cleaning, Principal Component Analysis(PCA)	–
[46]	365 blood images (dataset1), 242 blood images (dataset2)	Gram-Schmidt, Anisotropic Diffusion Filter (ADF), Self-dual Multi-scale Morphological Toggle Filter (SMMTF)	Similarity metrics: 90.1% (dataset1), 86.8% (dataset2)
[47]	Cervical cancer images	GMM, EM, MO, AIC, Hough transform	Recall: 94.9%, precision: 91.46%
[48]	265 ALL images, 150 blood images, 300 WBC images	MO, level set using geometric active contours	RI: 0.931

for Snakes to separate or segmentation in the case of multiple objects. Alternatively, the ACMs called Level Set is specifically designed to handle topological changes [13, 48, 55–61], but they are not robust to boundary haps and have other deficiencies as well [65]. The basic idea is to determine level curves from a potential function. These are iterative schemes thereby making computationally expensive to apply on large-scale histopathological images e.g. whole-slides. However, as can be seen in Table 5 active contours with level set implementations have been applied to nuclei segmentations.

3.2.5 Graph Cuts

Graph-based image segmentation approaches model one image as a weighted graph, in which each node associates a pixel or superpixels in the image and each edge weight between two nodes corresponds to the similarity between neighboring pixels of superpixels. According to a specific criterion, the graph is partitioned into multiple sets, each representing an object segment in the image [3]. Max-flow/min-cut algorithms have been widely applied to image segmentation in the field of computer visions and medical image analysis.

In graph Cuts algorithm, graphs are created from input images, and graph division is realized using max-flow/min-cut algorithm [40, 66, 67]. The graph consists of nodes corresponding to each pixel of the image, and terminals called source and sink. The edge connecting each node is called *n*-link, and the edge connecting source (S) and sink (T) terminals from each node is called t-link. The input object and background are called seed and the graph is divided into the object (nuclei), and the background by using max-flow/min-cut algorithms for the created graph. Details on graph cuts algorithm can be found in [68]. Table 6 provides a summary graph cut based methods for nuclei segmentation.

Table 5 Summary of active contours, level sets based nuclei segmentation methods for histopathological images

Refs.	Dataset	Preprocessing and segmentation	Segmentation results
[13]	234 H breast images	Level set based on interactive model	Precision: 0.90, recall: 0.78
[49]	100 H&E breast images	EM driven geodesic active contour with overlap resolution (EMaGACOR)	SEN: 80%, PPV: 86%
[50]	MITOS, renal cell carcinoma (RCC)	Localized active contour models	–
[51]	H&E bone marrow biopsy	Dual-channel ACM	Acc: $95.99 \pm 4.52\%$
[52]	668 rat kidney fluorescence microscopy images	3D active contours with inhomogeneity correction	Acc: 91.87% (DS-II), 89.65% (DS-III), 87.71% (DS-IV), 89.10% (DS-V)
[53]	30 H lung images	ACMs, 3D cell density estimation	Acc: 0.953 ± 0.017, 0.947 ± 0.016
[54]	Breast cancer images (MITOS)	Localized active contour models	–
[55]	44 H&E prostate images	Level sets	–
[56]	8 prostate images	Multiphase vector-based Level Set, FCM with spatial constraint	Precision: 84%, recall: 85%
[57]	Cervical Pap smear images	Level sets, Gaussian and Wiener filters	–
[58]	20 H&E breast images	Level set, 2D difference of Gaussian filter	–
[59]	180 cervical images	Median filter, Otsu thresholding, distance regularized level set evolution (DRLSE)	DC: 0.852 ± 0.076, TPR (pixel level): 0.885 ± 0.101, FPR (pixel level): 0.0015 ± 0.001, FNO (object level): 0.361 ± 0.158
[60]	Cervical Pap smear images	Level set, Gaussian and Wiener filters, Gray level co-occurrence matrix (GLCM)	–
[61]	89 H&E breast cancer slides	Level set which combines boundary and region information	–

Table 6 Summary of graph cut based nuclei segmentation methods for histopathological images

Refs.	Dataset	Preprocessing and segmentation	Segmentation results
[66]	440 H&E GBM images	Multi-reference GC (MRGC), LoG filter, GMM	Precistion: 0.75, recall: 0.85
[67]	450 fluorescence synthetic images	Distance-Map-Constrained Multiscale LoG filter, GC, iterative MO	CS: 89.37%, OS: 1.53%, US: 6.38%, Miss-seg: 0.83%, False-seg: 1.89%

Table 7 Summary of k-means clustering based nuclei segmentation methods for histopathological images

Refs.	Dataset	Preprocessing and segmentation	Segmentation results
[9]	1030 smear WBC images	HSI transform, k-means clustering	Neutrophil: 97.6%, Lymphocite: 97.0%, Monocyte: 97.8%, Eosinophil: 89.4%, Basophil: 89.7%
[69]	55 H&E prostate WSI	k-means clustering, entropy thresholding, multiscale difference of Gaussian	Acc: 97.6%
[70]	H&E lymphocyte images	Landmark based Spectral Clustering (LSC), Gabor filter	TPR: 80.70%, TNR: 94.37%, Acc rate: 92.49%, DC: 74.74
[71]	1030 smear WBC images	HSI transform, colour k-means clustering	Neutrophil: 93.6%, Lymphocite: 95.0%, Monocyte: 98.8%, Eosinophil: 90.4%, Basophil: 86.7%
[72]	85 H&E colon images	k-means clustering	–
[73]	Leukemia images	k-means clustering	–

3.2.6 K-Means Clustering

K-means clustering is one of the basic clustering techniques. and also, it is an iterative method used for partitioning the given image to K clusters (regions). Many techniques using K-means approach has been proposed like [9, 31, 41, 44, 69–74]. The basic algorithm of k-means is as follows.

a) Pick K cluster centers, either randomly or based on some heuristic.
b) Assign cluster label to each pixel in the image that minimizes the distance between the pixel and the cluster center.
c) Recompute the cluster centers by averaging all the pixels in the cluster.
d) Repeat steps b) and c) until convergence is attained or no pixel changes its cluster.

In basic k-means clustering techniques, Euclidean distance is usually used for the distance between the cluster center and the data when the cluster is comparatively isotropy. As more highly technique, fuzzified k-means clustering method "Fuzzy c-means" is sometimes used. The fuzzy c-means method uses possibilities that shows how the clusters overlap each other for clustering. The nuclei segmentation using k-means clustering method are proposed in [75, 76]. The segmentation method using superpixel algorithm is also proposed, and these are called simple linear iterative clustering (SLIC) [77, 78]. For instance, Cheikh et al. [77] applied the SLIC approach, that clusters pixels in the five-dimensional color and image plane space to efficiently generate compact, nearly uniform small regions. The result of their approach using the SLIC algorithm was better than watershed-based methods. The differences are typically based on the pixel value, texture, and location, or a weighted combination of these factors. Its robustness depends mainly on the initialization of clusters [3]. Table 7 details the k-means clustering based approaches applied to nuclei segmentation.

3.2.7 Segmentation with Deep Learning Techniques

Deep learning is based on artificial neural networks (ANN) which is a system imitating the mechanism of human nerve cells (neurons). Although the performance of deep learning approaches heavily depends on the number of learning data, the algorithm of deep learning is generally smart compared to other methods. In these years, this approach is often used for automatic classification and segmentation, Fig. 3. The algorithm can classify and segment by learning features

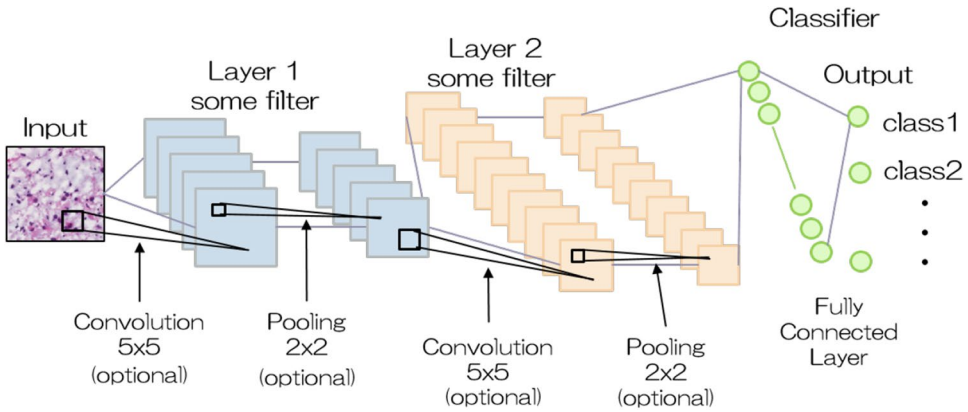

Fig. 3 An example of convolutional neural network (CNN) architecture used in [81]

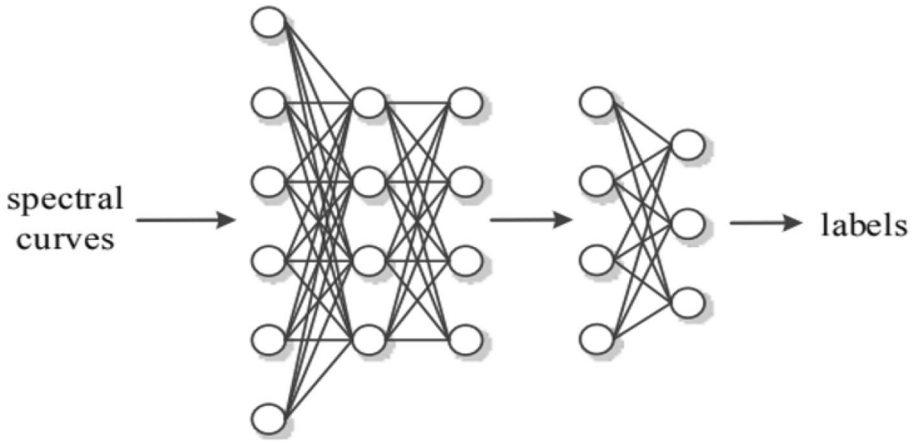

Fig. 4 Deep belief network (DBN) architecture used in [80]

from mass data, and several methods have already been established. These methods are introduced in literature [79].

Deep Belief Network (DBN) [80], Fig. 4, was developed as one of the methods of deep learning. After this, various architectures such as Stacked Auto Encoder (SAE) and Convolutional Neural Network (CNN) appeared. CNN is the common and worldwide neural network method for image processing. CNN has obtained great success in various tasks of computer vision and biomedical image analyses. Generally, when we use traditional and typical neural networks and handle two-dimensional (matrix) data like an image, the data structure should be converted into one-dimensional (vector) data for learning. On the other hand, since CNN can handle the two-dimensional data as learning data, it is expected that CNN works well the data that has information of positional relationship(s). Figure 3 illustrates an example of the basic architecture of CNN. CNN consists of convolution layer(s) and pooling layer(s). The convolution layer compresses the features in small area of the given image, and the pooling layer generates new feature maps obtained by the convolutional operation.

In [82–87], the authors used CNN approach for nuclei segmentation and classification. For instance, Kumar et al. [82] presented a detection method of boundary using three-class CNN (CNN3) for touching nuclei. In the literature, they used *The Cancer Genome Atlas* (TCGA) to make experimental materials [88]. They carried out color normalization as preprocessing. By adding the third class, it is possible to find inter-nuclear boundaries irrespective of the configuration of the crowded nuclei.

Isaksson et al. [84] proposed semantic nuclei segmentation method using CNN. Figure 5 shows their network design. Due to the limitation of the number of annotated data, they chose to expand it artificially using data augmentation. The data augmentation is used for rotation, enlargement, and reduction when the experimental data is not enough. In [85], Fu et al. also used data augmentation for their experiment. Consequently, Isaksson et al. [84] got a segmentation accuracy of 78%.

Recently, segmentation and classification using deep learning approaches are used widely to obtain state-of-the-art for disease analysis and diagnosis in various biomedical imaging domains. As can be seen in Table 8, CNN models obtain good nuclei segmentations across datasets in H&E stained images with consistently high accuracy. However, the interpretability of such deep CNN models is not easy and despite the adaptability across datasets, deep learning models still require fair bit of training that in turn requires

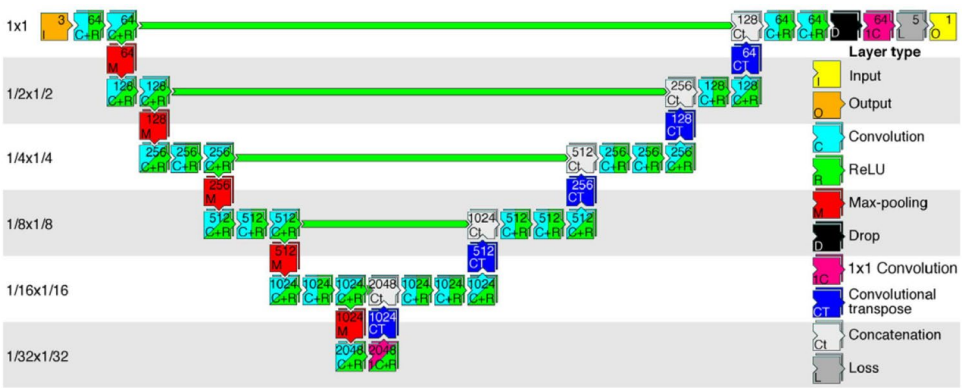

Fig. 5 CNN design used in [84], which was based on the U-Net model

Table 8 Summary of machine learning (deep learning) based nuclei segmentation methods for histopathological images

Refs.	Dataset	Preprocessing and segmentation	Segmentation results
[82]	30 breast, kidney, liver, and prostate WSIs	Deep learning, CNN	92%
[83]	31 brain, 51 NET, and 35 breast cancer images	CNN, iterative region merging, local repulsive deformable model	Mean dice values, brain: 0.85, NET: 0.92, breast cancer: 0.80
[84]	H&E prostate images	CNN, deep learning	78%
[85]	Rat kidney fluorescence images	Deep CNN	Dataset1, 2, 3: 94.25, 95.24, 93.21%
[89]	33 H&E breast images	Deep neural network	Acc: 94.4%
[86]	917 Pap smear images, H&E cervical images	CNN	Sen: 98.2 $\pm$ 1.2%, Acc: 98.3 $\pm$ 0.3%
[87]	U2OS, NIH3T3	Deep CNN	U2OS/NIH3T3 (1,2,4 and 8 frames) RI: 97% (1, 2, 4 and 8)/87, 89, 91, 92%

high computational cost. Nevertheless, using deep learning models and especially CNN models are useful in avoiding adhoc filtering, thresholding and feature selection steps in the previous nuclei segmentation techniques surveyed. We also note the lack of large-scale histopathological datasets dedicated to nuclei segmentations benchmarking, and current deep learning models require domain related training data in achieving higher accuracy.

4 Discussion and Conclusion

Since late 1990's, research projects on nuclei segmentation have been reported, but the number of the published papers is not many because the digital equipment was accessible in the limited medical/clinical areas. Thanks to the recent developments in digital pathology, a lot of methods for cancer detection and grading approaches have been proposed. Accordingly, the number of published papers on nuclei segmentation methods has been increasing. However, most of the studies use their in-house datasets as experimental materials. Of course, there are various image modalities, staining method, and it is impossible to do in the same condition. Therefore, evaluation criteria depends on pathologists. Due to this reason, evaluating the obtained results may or may not be correct. To evaluate the performance of these methods under the same condition, we need public datasets for histopathological image processing and analysis. Currently, there are several public datasets for nuclei/cell detection and segmentation approaches, but they cannot cover all situation completely. More datasets will be required to expand the field of histopathological image processing and analysis.

We should also address the development of a more robust method that can be used with different staining, scanner, lighting conditions, and magnifications. Segmentation methods such as thresholding, region growing, and watershed approaches can locate cell nuclei but do not work well when they try to segment the touching and overlapping nuclei. Deep learning based on neural networks are well-suited to tackle nuclei segmentation under complex conditions. Due to the lack of availability of large-scale labeled data in the histopathological community, crowd-sourced or generative adversarial networks (GANs) based approaches can be employed. We envisage top performing deep learning models, in particular, methods based on the already successful CNNs can further be expanded to include domain-specific priors for improving the histopathological nuclei segmentation.

It is still one of the hot topics for nuclei segmentation to deal with overlapped and clustered nuclei. Several methods for the challenges have been proposed so far, but the problem has not been completely solved yet. The methods such as thresholding [25, 32, 33], marker-controlled watershed [34, 35], level set [13, 59], graph cut [67] approaches have been developed to separate overlapping, touching and clustered nuclei. By using these methods, cell nuclei that are slightly touching/overlapping can be separated, but they sometimes do not work well when there are many touching/overlapping nuclei in the given image. Also, these methods are not suitable for large scale nuclei segmentation, for example in whole-slide images. For instance, when we use marker-controlled watershed, true nuclei markers are needed. ACMs, clustering and graph-based methods may need plenty of computational costs when applying to WSI. Therefore, the demand for establishing a robust nuclei segmentation method, which is adaptable to WSI and a large number of overlapping and touching nuclei, will be grown in the field of image analysis for digital pathology and microscopy images.

Compliance with Ethical Standards

Conflict of interest On behalf of all authors, the corresponding author states that there is no conflict of interest.

References

1. Irshad H et al (2014) Methods for nuclei detection, segmentation, and classification in digital histopathology: a review—current status and future potential. IEEE Rev Biomed Eng 7:97–114
2. Gurcan MN et al (2009) Histopathological image analysis: a review. IEEE Rev Biomed Eng 2:147–171
3. Xing F, Yang L (2016) Robust nucleus/cell detection and segmentation in digital pathology and microscopy images: a comprehensive review. IEEE Rev Biomed Eng 9:234–263
4. Cheng F-H, Hsu N-R (2016) Automated cell nuclei segmentation from microscopic images of cervical smear. In: 2016 international conference on applied system innovation (ICASI). IEEE
5. Jing J et al (2016) An improved hybrid active contour model for nuclear segmentation on breast cancer histopathology. In: 2016 IEEE 13th international symposium on biomedical imaging (ISBI). IEEE
6. Mansoori T et al (2007) An iterative method for registration of high-resolution cardiac histoanatomical and MRI images. In: 4th IEEE international symposium on biomedical imaging: from nano to macro, 2007. ISBI 2007. IEEE
7. Guo P, Evans A, Bhattacharya P (2016) Segmentation of nuclei in digital pathology images. In: 2016 IEEE 15th international conference on cognitive informatics & cognitive computing (ICCI*CC). IEEE
8. Manik S, Saini LM, Vadera N (2016) Counting and classification of white blood cell using artificial neural network (ANN). In: IEEE international conference on power electronics, intelligent control and energy systems (ICPEICES). IEEE, 2016
9. Sajjad M et al (2017) Leukocytes classification and segmentation in microscopic blood smear: a resource-aware healthcare service in smart cities. IEEE Access 5:3475–3489
10. Al-Kofahi Y, Lassoued W et al (2010) Improved automatic detection and segmentation of cell nuclei in histopathology images. IEEE TBE 57(4):841–852
11. Xu H et al (2017) Automatic nuclear segmentation using multi-scale radial line scanning with dynamic programming. IEEE Trans Biomed Eng 64(10):2475–2485
12. Parvin B et al (2007) Iterative voting for inference of structural saliency and characterization of subcellular events. IEEE Trans Image Process 16(3):615–623
13. Qi X, Xing F et al (2012) Robust segmentation of overlapping cells in histopathology specimens using parallel seed detection and repulsive level set. IEEE TBE 53(3):754–765
14. Hamilton PW et al (1997) Automated location of dysplastic fields in colorectal histology using image texture analysis. J Pathol 182(1):68–75
15. Khan AM, El-Daly H, Simmons E, Rajpoot NM (2013) HyMaP: a hybrid magnitude-phase approach to unsupervised segmentation of tumor areas in breast cancer histology images. J Pathol Inform. https://doi.org/10.4103/2153-3539.109802
16. Lee HG, Lee SC (2017) Nucleus segmentation using Gaussian mixture based shape models. IEEE J Biomed Health Inform 22(1):235–243
17. Otsu N (1975) A threshold selection method from gray-level histograms. Automatica 11(285–296):23–27
18. Lu C, Mahmood M, Jha N, Mandal M (2012) A robust automatic nuclei segmentation technique for quantitative histopathological image analysis. AQCH 34:296–308
19. Ortiz De Solrzano C et al (1999) Segmentation of confocal microscope images of cell nuclei in thick tissue sections. J Microsc 193(3):212–226
20. Gadgil NJ et al (2016) Nuclei segmentation of fluorescence microscopy images based on midpoint analysis and marked point process. In: 2016 IEEE southwest symposium on image analysis and interpretation (SSIAI). IEEE
21. Slavkovi-Ili MS, Paska MP, Reljin BD (2016) Nuclei segmentation from contrast enhanced FISH images. In: 2016 13th symposium on neural networks and applications (NEUREL). IEEE
22. Win KY, Choomchuay S (2017) Automated segmentation of cell nuclei in cytology pleural fluid images using Otsu thresholding. In: International conference on digital arts, media and technology (ICDAMT). IEEE
23. Ahasan R, Ratul AU, Bakibillah ASM (2016) White blood cells nucleus segmentation from microscopic images of strained peripheral blood film during leukemia and normal condition. In: 2016 5th international conference on informatics, electronics and vision (ICIEV). IEEE
24. Phoulady HA et al (2016) Automatic quantification and classification of cervical cancer via adaptive nucleus shape modeling. In: 2016 IEEE international conference on image processing (ICIP). IEEE, 2016
25. Lee H, Kim J (2016) Segmentation of overlapping cervical cells in microscopic images with superpixel partitioning and cell-wise contour refinement. In: Proceedings of the IEEE conference on computer vision and pattern recognition workshops
26. Fukuma K et al (2016) A study on feature extraction and disease stage classification for glioma pathology images. In: 2016 IEEE international conference on fuzzy systems (FUZZ-IEEE). IEEE
27. Gautam A et al (2016) Automatic classification of leukocytes using morphological features and Nave Bayes classifier. In: 2016 IEEE region 10 conference (TENCON). IEEE
28. Sazzad TMS, Armstrong LJ, Tripathy AK (2016) An automated ovarian tissue detection approach using type P63 non-counter stained images to minimize pathology experts observation variability. In: 2016 IEEE EMBS conference on biomedical engineering and sciences (IECBES). IEEE
29. Tareef A et al (2016) Automatic nuclei and cytoplasm segmentation of leukocytes with color and texture-based image enhancement. In: 2016 IEEE 13th international symposium on biomedical imaging (ISBI). IEEE
30. Vinothini A, Prasad B (2016) Segmentation of clusters nuclei based on intensity and texture in phase contrast image using h-maxima transformation. In: International conference on wireless communications, signal processing and networking (WiSPNET). IEEE
31. Anishiya P, Sasikala M (2016) Segmentation and localization of epithelial cells in the histopathological images of stomach adenocarcinoma. In: International conference on wireless communications, signal processing and networking (WiSPNET). IEEE
32. Phoulady HA et al (2016) A new approach to detect and segment overlapping cells in multi-layer cervical cell volume images. In: 2016 IEEE 13th international symposium on biomedical imaging (ISBI). IEEE
33. Hou L et al (2016) Automatic histopathology image analysis with CNNs. In: Scientific data summit (NYSDS), 2016 New York. IEEE
34. Veta M, van Diest PJ et al (2013) Automatic nuclei segmentation in H&E stained breast cancer histopathology images. PLoS ONE 8(7):e70221
35. Veta M, Huisman A et al (2011) Marker-controlled watershed segmentation of nuclei in H&E stained breast cancer biopsy images. In: IEEE ISBI, pp 618–621
36. Shu J, Fu H et al (2013) Segmenting overlapping cell nuclei in digital histopathology images. In: 2013 35th annual international conference of the IEEE engineering in medicine and biology society (EMBC). IEEE
37. Kost H, Homeyer A, Molin J, Lundström C, Hahn HK (2017) Training nuclei detection algorithms with simple annotations. J Pathol Inform 8:21

38. Rajyalakshmi U, Rao SK, Prasad KS (2017) Supervised classification of breast cancer malignancy using integrated modified marker controlled watershed approach. In: 2017 IEEE 7th international advance computing conference (IACC). IEEE
39. Cui Y, Hu J (2016) Self-adjusting nuclei segmentation (SANS) of Hematoxylin-Eosin stained histopathological breast cancer images. In: 2016 IEEE international conference on bioinformatics and biomedicine (BIBM). IEEE
40. Nandy K et al (2016) Segmentation of nuclei from 3D microscopy images of tissue via graphcut optimization. IEEE J Sel Topics Signal Process 10(1):140–150
41. Shi P et al (2016) Automated quantitative image analysis of Hematoxylin-Eosin staining slides in lymphoma based on hierarchical kmeans clustering. In: 2016 8th international conference on information technology in medicine and education (ITME). IEEE
42. Roerdink JBTM, Arnold M (2000) The watershed transform: definitions, algorithms and parallelization strategies. Fundamenta Informaticae 41.1(2):187–228
43. Sokol P, Garcia FU et al (2006) Large-scale computations on histology images reveal grade-differentiating parameters for breast cancer. BMC Med Imaging 6:14
44. Neghina M et al (2016) Automatic detection of cervical cells in Pap-smear images using polar transform and k-means segmentation. In: 2016 6th international conference on image processing theory tools and applications (IPTA). IEEE
45. Zarei N et al (2017) Automated prostate glandular and nuclei detection using hyperspectral imaging. In: 2017 IEEE 14th international symposium on biomedical imaging (ISBI 2017). IEEE
46. Tareef A et al (2017) Automated multi-stage segmentation of white blood cells via optimizing color processing. In: 2017 IEEE 14th international symposium on biomedical imaging (ISBI 2017). IEEE
47. Ragothaman S et al (2016) Unsupervised segmentation of cervical cell images using Gaussian mixture model. In: Proceedings of the IEEE conference on computer vision and pattern recognition workshops
48. Al-Dulaimi K et al (2016) White blood cell nuclei segmentation using level set methods and geometric active contours. In: 2016 international conference on digital image computing: techniques and applications (DICTA). IEEE
49. Fatakdawala H, Xu J et al (2010) Expectation–maximization-driven geodesic active coutour with overlap resolution(EMaGACOR): application to lymphocyte segmentation on breast cancer histopathology. IEEE TBE 57(7):1676–1689
50. Sabeena K, Nair MS, Bindu GR (2017) A multi-classifier system for automatic mitosis detection in breast histopathology images using deep belief networks. IEEE J Transl Eng Health Med 5:1–11
51. Song T-H et al (2017) Dual-channel active contour model for megakaryocytic cell segmentation in bone marrow trephine histology images. IEEE Trans Biomed Eng 64:2913–2923
52. Lee S et al (2017) Segmentation of fluorescence microscopy images using three dimensional active contours with inhomogeneity correction. In: 2017 IEEE 14th international symposium on biomedical imaging (ISBI 2017). IEEE
53. Yin Y et al (2017) Tumor cell load and heterogeneity estimation from diffusion-weighted MRI calibrated with histological data: an example from lung cancer. IEEE Trans Med Imaging 37:35–46
54. Beevi KS, Nair MS, Bindu GR (2016) Detection of mitotic nuclei in breast histopathology images using localized ACM and random kitchen sink based classifier. In: 2016 IEEE 38th annual international conference of the engineering in medicine and biology society (EMBC). IEEE
55. Naik S, Doyle S et al (2007) Gland segmentation and computerized Gleason grading of prostate histology by integrating low-, high-level and domain specific information. In: MIAAB workshop
56. Hafiane A, Bunyak F, Palaniappan K (2008) Fuzzy clustering and active contours for histopathology image segmentation and nuclei detection. In: ACIVS, pp 903–914
57. Kashyap D et al (2016) Cervical cancer detection and classification using independent Level sets and multi SVMs. In: 2016 39th international conference on telecommunications and signal processing (TSP). IEEE
58. Faridi P et al (2016) An automatic system for cell nuclei pleomorphism segmentation in histopathological images of breast cancer. In: 2016 IEEE signal processing in medicine and biology symposium (SPMB). IEEE
59. Kumar P et al (2016) An unsupervised approach for overlapping cervical cell cytoplasm segmentation. In: 2016 IEEE EMBS conference on biomedical engineering and sciences (IECBES). IEEE
60. Bhan A, Vyas G, Mishra S (2016) Supervised segmentation of overlapping cervical pap smear images. In: 2016 international conference on signal processing and communication (ICSC). IEEE
61. Cao J et al (2016) An automatic breast cancer grading method in histopathological images based on pixel-, object-, and semantic-level features. In: 2016 IEEE 13th international symposium on biomedical imaging (ISBI). IEEE
62. Kass M, Witkin A, Terzopoulos D (1988) Snakes: active contour models. Int J Comput Vis 1(4):321–331
63. Street WN, Wolberg WH, Mangasarian OL (1993) Nuclear feature extraction for breast tumor diagnosis. In: Biomedical image processing and biomedical visualization, vol 1905. International Society for Optics and Photonics
64. Roula MA, Bouridane A, Kurugollu F (2004) An evolutionary snake algorithm for the segmentation of nuclei in histopathological images. In: 2004 international conference on image processing, 2004. ICIP'04, vol 1. IEEE, pp 127–130
65. Jasjit JS (2002) Shape recovery algorithms using level sets in 2-D/3-D medical imagery: a state-of-the-art review. IEEE Trans Inf Technol Biomed 6.1:8–28
66. Chang H, Loss LA, Parvin B (2012) Nuclear segmentation in H&E sections via multi-reference graph cut (MRGC). In: International symposium biomedical imaging
67. Song J, Xiao L, Lian Z (2015) Boundary-to-marker evidence controlled segmentation and MDL-based contour inference for overlapping nuclei. IEEE J Biomed Health Inform 21:451–464
68. Nagahashi T, Hujiyoshi H, Kanada T (2008) Image segmentation using iterated graph cuts based on multi-scale smoothing. CVIM 1(2):10–20
69. Niazi MKK et al (2017) Visually meaningful histopathological features for automatic grading of prostate cancer. IEEE J Biomed Health Inform 21(4):1027–1038
70. Chang YH et al (2016) Quantitative analysis of histological tissue image based on cytological profiles and spatial statistics. In: 2016 IEEE 38th annual international conference of the engineering in medicine and biology society (EMBC). IEEE
71. Sajjad M et al (2016) Computer aided system for leukocytes classification and segmentation in blood smear images. In: 2016 international conference on frontiers of information technology (FIT). IEEE
72. Nateghi R, Danyali H, Helfroush M-S (2016) A systematic approach for glandular structure segmentation from colon histopathology images. In: 2016 24th Iranian conference on electrical engineering (ICEE). IEEE
73. Rejintal A, Aswini N (2016) Image processing based leukemia cancer cell detection. In: IEEE international conference on recent trends in electronics, information & communication technology (RTEICT). IEEE

74. MacQueen J (1967) Some methods for classification and analysis of multivariate observations. In: Proceedings of the fifth Berkeley symposium on mathematical statistics and probability, vol 1(14)
75. Sharma B, Mangat KK (2016) An improved nucleus segmentation for cervical cell images using FCM clustering and BPNN. In: 2016 international conference on advances in computing, communications and informatics (ICACCI). IEEE
76. Saha R, Bajger M, Lee G (2016) Spatial shape constrained fuzzy c-means (FCM) clustering for nucleus segmentation in pap smear images. In: 2016 international conference on digital image computing: techniques and applications (DICTA). IEEE
77. Cheikh BB et al (2017) Spatial interaction analysis with graph based mathematical morphology for histopathology. In: 2017 IEEE 14th international symposium on biomedical imaging (ISBI 2017). IEEE
78. Oliveira PHC et al (2017) A multi-objective approach for calibration and detection of cervical cells nuclei. In: 2017 IEEE congress on evolutionary computation (CEC). IEEE
79. Xing F et al (2017) Deep learning in microscopy image analysis: a survey. IEEE Trans Neural Netw Learn Syst 29:4550–4568
80. Li T, Zhang J, Zhang Y (2014) Classification of hyperspectral image based on deep belief networks. In: 2014 IEEE international conference on image processing (ICIP). IEEE
81. Yonekura A, Kawanaka H, Prasath VBS, Aronow BJ, Takase H (2018) Automatic disease stage classification of glioblastoma multiforme histopathological images using deep convolutional neural network. Biomed Eng Lett 8(3):321–327
82. Kumar N et al (2017) A dataset and a technique for generalized nuclear segmentation for computational pathology. IEEE Trans Med Imaging 36:1550–1560
83. Xing F, Xie Y, Yang L (2016) An automatic learning-based framework for robust nucleus segmentation. IEEE Trans Med Imaging 35(2):550–566
84. Isaksson J et al (2017) Semantic segmentation of microscopic images of H&E stained prostatic tissue using CNN. In: 2017 international joint conference on neural networks (IJCNN). IEEE
85. Fu C et al (2017) Nuclei segmentation of fluorescence microscopy images using convolutional neural networks. In: 2017 IEEE 14th international symposium on biomedical imaging (ISBI 2017). IEEE
86. Zhang L et al (2017) DeepPap: deep convolutional networks for cervical cell classification. IEEE J Biomed Health Inform 21:1633–1643
87. Huang JY, Hughes NJ, Goodhill GJ (2016) Segmenting neuronal growth cones using deep convolutional neural networks. In: 2016 international conference on digital image computing: techniques and applications (DICTA). IEEE
88. The Cancer Genome Atlas. https://cancergenome.nih.gov/
89. Naylor P et al (2017) Nuclei segmentation in histopathology images using deep neural networks. In: 2017 IEEE 14th international symposium on biomedical imaging (ISBI 2017). IEEE